

Magnetic springs in exchange-coupled DyFe₂/YFe₂ superlattices: An element-selective x-ray magnetic circular dichroism study

K. Dumesnil, C. Dufour, and Ph. Mangin

*Laboratoire de Physique des Matériaux (UMR CNRS 7556), Université H. Poincaré, Nancy I, BP 239,
54506 Vandoeuvre les Nancy cedex, France*

A. Rogalev

ESRF, BP 220, 38043 Grenoble cedex, France

(Received 15 May 2001; published 31 January 2002)

X-ray magnetic circular dichroism technique has been exploited to measure material-selective hysteresis loops in DyFe₂/YFe₂ exchange-coupled superlattices. The magnetization reversal in these systems depends strongly on the individual thickness of both compounds. In superlattices with 100-Å-thick DyFe₂ layers, recall springs are shown to develop in the soft YFe₂ layers, as expected from the domain wall energy values. On the contrary, when the DyFe₂ layers are thinner, the YFe₂ magnetization remains aligned along the field direction and the DyFe₂ net magnetization rotates due to the interface exchange interaction. This observation proves that magnetic exchange springs penetrate into the magnetically hard DyFe₂ layers.

DOI: 10.1103/PhysRevB.65.094401

PACS number(s): 75.60.-d, 75.25.+z, 75.70.Cn, 71.20.Eh

The DyFe₂/YFe₂ superlattices composed of hard and soft magnetic materials of high crystallographic quality are representative examples of interface exchange-coupled systems. These complex magnetic heterostructures belong to a very promising category of spring magnets ($R\text{Fe}_2/R^*\text{Fe}_2$), in which R is a highly anisotropic rare-earth metal (Dy-Tb-Sm-Er-Nd) and R^* is a nonmagnetic rare-earth element (Y, La, Lu) or an almost isotropic metal, such as Gd.¹⁻⁴ They also exhibit an exchange bias effect that is either positive or negative, showing memory of the field history of the superlattice.¹ These two latter effects (exchange spring and exchange bias) are currently a matter of high interest^{5,6} for both fundamental and technological reasons, because they are central issues for permanent magnet and spin-valve devices. A detailed understanding of the magnetization reversal process, strongly related to exchange coupling effects at the interfaces, is therefore highly desirable.

Various studies have been carried out on the preparation and on the magnetic properties of single-crystalline $R\text{Fe}_2$ thin films.⁷⁻¹¹ In particular, they have elucidated the key role played by the epitaxial strains in the spontaneous magnetization direction caused by the strong magnetoelastic coupling. In $R\text{Fe}_2/R^*\text{Fe}_2$ superlattices, the iron atoms are coupled ferromagnetically at the interfaces as well as in the layers. Depending on the relative orientation of the net magnetization of the layers and of the iron sublattice, the coupling between the layers can be either ferromagnetic or antiferromagnetic. Recently, extensive studies of the magnetic behavior of DyFe₂/YFe₂ (110) superlattices have been initiated.^{1,4} YFe₂ is a soft ferromagnet, whereas DyFe₂ is a hard magnetic material (the anisotropy constants K_1 in these compounds are respectively close to 10^6 erg/cm³ and 4×10^7 erg/cm³ at room temperature). In DyFe₂, the Dy magnetic moments are dominant and antiferromagnetically coupled to the iron ones. At the DyFe₂/YFe₂ interface, the coupling between net magnetization of both layers is therefore antiferromagnetic. Up to now, the magnetic configurations occurring under magnetic

field have been only deduced from macroscopic magnetization measurements that give the total magnetization from the whole superlattice. The mechanism of magnetization reversal is relatively well understood in the case of thick layers of both materials: the magnetization of the hard material is defined by the crystal field anisotropy, whereas interface domain walls develop in the soft material and act as recall springs.^{1,4} For thin DyFe₂ layers the magnetic behavior of the superlattices is by far more complex, especially at high temperatures (above 100 K). To unravel the underlying mechanism one needs to exploit an experimental technique which probes the magnetic properties of each compound independently.

To go further in our studies of the exchange coupling phenomena in DyFe₂/YFe₂ superlattices, we have investigated compound-resolved magnetization reversal using x-ray magnetic circular dichroism (XMCD) which was proved to be the element- and orbital-selective magnetometry tool.¹² We performed XMCD measurements on two DyFe₂/YFe₂ superlattices, with 100-Å-thick and 50-Å-thick DyFe₂ layers. Monitoring the XMCD signal at the Dy L_3 ($2p$ - $5d$ transitions) and Y L_3 ($2p$ - $4d$ transitions) absorption edges as a function of applied magnetic field, we were able to record element-specific, and thus compound-selective, hysteresis loops.

The XMCD spectra at these edges are related to the induced magnetic moments of the Dy $5d$ and Y $4d$ states, whereas the magnetism of the compounds is dominated by Dy $4f$ and Fe $3d$ states. The polarization of the Dy $5d$ and Y $4d$ shells is, however, proportional to the total magnetization in the DyFe₂ and YFe₂ layers respectively. Thus the field dependence of the XMCD signals is directly related to the field dependence of the magnetization of the specified compound, projected onto the direction of the incident x rays (i.e., of the external magnetic field).

The samples were prepared following the process developed for the epitaxial growth of single-crystalline (110) $R\text{Fe}_2$

thin films, described in Ref. 7. *In situ* reflection high-energy electron diffraction (RHEED) observations, as well as large-angle x-ray scattering experiments, evidence the high single-crystal quality of these composite systems.¹ Several superlattice satellites around the main (110) Bragg reflection reveal the periodic stacking of DyFe₂ and YFe₂ layers. The two superlattices measured for this study are [DyFe₂(100 Å)/YFe₂(130 Å)]₁₈ and [DyFe₂(50 Å)/YFe₂(130 Å)]₂₁, referred to as sample I and II, respectively, in the following. The x-ray magnetic circular dichroism experiments were performed at the European Synchrotron Radiation Facility (ESRF) in Grenoble (France) on the ID12A beamline.¹³ The applied magnetic field (up to ± 7 T) was parallel to the direction of the incident x-ray beam. In order to apply the magnetic field as close as possible to the easy magnetization direction of the samples (the in-plane $[1\bar{1}0]$ direction¹¹), we used a specific sample holder that permitted a grazing incidence geometry, where the incident beam and the magnetic field are at 5° from this in-plane $[1\bar{1}0]$ direction. The XMCD spectra were recorded by flipping the helicity of incoming x rays and keeping the direction of the magnetic field fixed. For the experiments at the Y L₃ edge, we used the fundamental harmonic of a hybrid electromagnetic helical undulator (EMPHU),¹⁴ which allowed us to flip the helicity of x rays at every energy point of the scan. While for the XMCD measurements at the Dy L₃, the second harmonic of the HELIOS-II undulator has been used and the helicity of incoming photons was changed after each consecutive energy scan. In both cases the degree of circular polarization of the monochromatic x-ray beam was estimated to be in excess of 85%. The spectra were recorded in the total fluorescence detection mode, which is not sensitive to the external applied magnetic field, at least in the range of interest (+7 to -7 T).

Typical XMCD spectra at both Dy and Y edges are shown in Fig. 1 (left scales), together with the normalized x-ray absorption spectra (right scales). To record the element-selective hysteresis curves, the energy of the incident x-ray photons was tuned to the maximum of the XMCD signal either at the Dy L₃ absorption edge (7.789 keV) or at the Y L₃ edge (2.08 keV). The amplitude of the dichroic signal at each value of the applied magnetic field was measured by flipping the helicity of the x-ray beam. The hysteresis loops measurements have been done at the Dy L₃ edge for sample I and at both the Dy and Y L₃ edges for sample II.

The XMCD signal collected at the Dy L₃ edge versus the applied magnetic field for sample [DyFe₂(100 Å)/YFe₂(130 Å)]₁₈ is shown in Fig. 2 (solid circles) at 100 and 200 K. As presented in Ref. 1, these temperatures are the most characteristic of the magnetic behavior over the whole temperature range. The measured loops are correlated to the magnetic behavior of DyFe₂ magnetization. The loops presented with solid curves correspond to the macroscopic magnetization measurements performed with a superconducting quantum interference device (SQUID) magnetometer, and thus reveal the magnetic behavior from the whole sample (DyFe₂ and YFe₂). At both temperatures, the XMCD signal exhibits almost square loops, whose coercive fields H_c (3.2 T

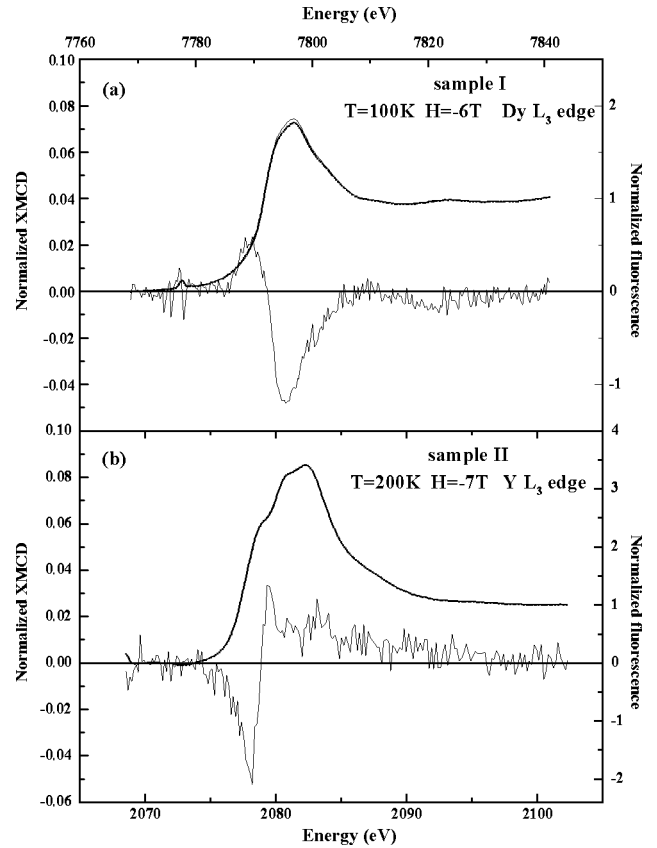


FIG. 1. Normalized x-ray magnetic circular dichroic signal and normalized x-ray appearance near-edge structure (XANES) spectra measured using total fluorescence yield (a) at 100 K, under a -6 T external magnetic field and around the Dy L₃ edge for the sample [DyFe₂(100 Å)/YFe₂(130 Å)]₁₈ (b) at 200 K, under a -7 T external magnetic field and around the Y L₃ edge for the sample [DyFe₂(50 Å)/YFe₂(130 Å)]₂₁.

at 100 K and 2 T at 200 K) are precisely at the field where the total magnetization abruptly drops (increases) towards saturation along the applied negative (positive) field. This means that, as expected from the strong anisotropy in DyFe₂, the magnetization of the DyFe₂ layers is almost constant before switching sharply at H_c . Note, however, a slight reduction in the DyFe₂ magnetization prior the reversal, especially at 200 K where the anisotropy is smaller. This should be due to a shift of the magnetization from the easy direction. In comparing XMCD measurements at the Dy L₃ edge and SQUID measurements, one can thus conclude that the less sharp variation in magnetization measured for positive decreasing fields must be attributed to the YFe₂ magnetization. The successive magnetic configurations can be described as follows: at +7 T, the net magnetization of both compounds is along the external field with thin domain walls at the interfaces in the YFe₂ layers. From +7 T to 0, the domain walls decompress and extend so that the magnetization of YFe₂ progressively orientates along the iron moments in DyFe₂ (i.e., along the negative fields). From 0 to $-H_c$ the sample is ferrimagnetic and, at $-H_c$, the magnetization of DyFe₂ switches with again the formation of domain walls in the soft YFe₂ layers, which become thinner and thinner as the field

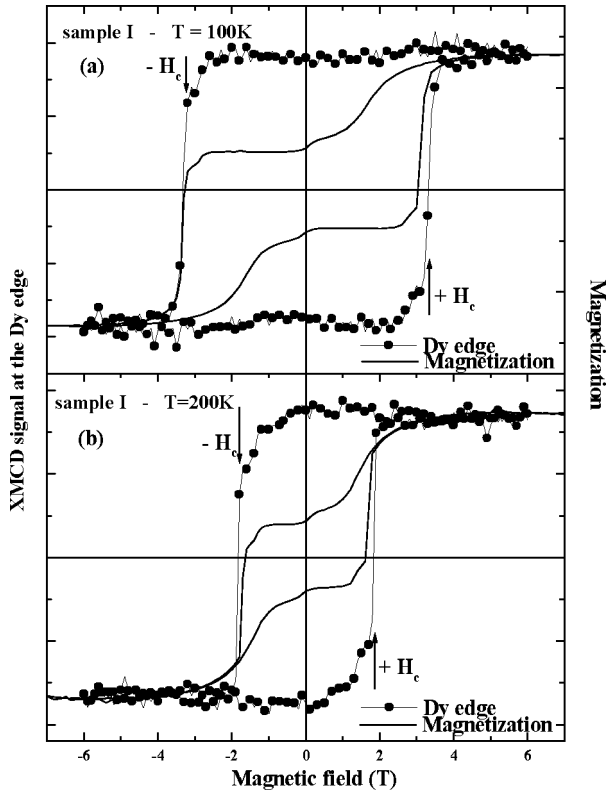


FIG. 2. Hysteresis loops measured at 100 and 200 K for the superlattice $[\text{DyFe}_2(100 \text{ \AA})/\text{YFe}_2(130 \text{ \AA})]_{18}$. The results presented with black dots correspond to the Dy XMCD signal and reveal the magnetic behavior of the DyFe_2 layers. The results presented with solid curves correspond to SQUID measurements and reveal the magnetic behavior from the whole sample.

becomes more negative. This is the standard description of the behavior of a spring magnet with antiferromagnetic exchange coupling at the interfaces. Note the small jump in the magnetization as the magnetic field passes through zero that has been also observed by other authors. An interpretation has been given in Ref. 10 and the problem has been briefly discussed by Sawicki *et al.*⁴ From other samples that were fabricated with different capping layers, we believe that this feature could be due to oxidation.

The XMCD signals versus external magnetic field measured at the Dy and Y L_3 edges (solid and open circles, respectively) are shown in Fig. 3 for the superlattice $[\text{DyFe}_2(50 \text{ \AA})/\text{YFe}_2(130 \text{ \AA})]_{21}$. The XMCD study has been focused on the high-temperature range (200 and 250 K), because the low-temperature behavior appears to be rather simple and could be elucidated from classical SQUID measurements.¹ The behavior of the DyFe_2 magnetization (deduced from the Dy dichroic signal) can be compared at 200 K to the previous sample: in this superlattice where the DyFe_2 layers are twice thinner, the loop is not square at all, which means that the magnetization reversal occurs in a completely different way and cannot be interpreted so simply. When decreasing the magnetic field, the magnetization reversal occurs in three stages, at both temperatures: (i) from +7 to +1 T, the Dy signal decreases continuously, whereas the Y signal remains almost constant at $+Y_{\text{max}}$, (ii)

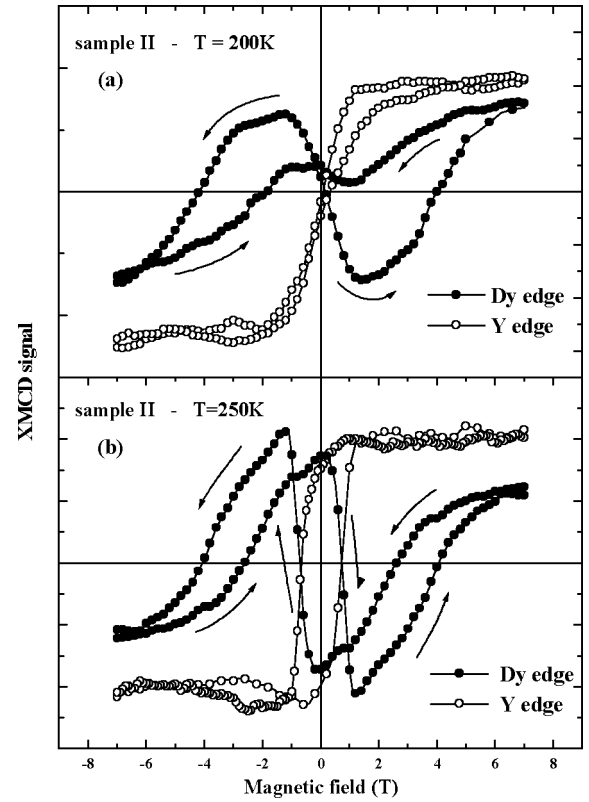


FIG. 3. Hysteresis loops measured by XMCD at 200 and 250 K for the superlattice $[\text{DyFe}_2(50 \text{ \AA})/\text{YFe}_2(130 \text{ \AA})]_{21}$. The results presented with solid circles correspond to the Dy XMCD signal and reveal the magnetic behavior of the DyFe_2 layers. The results presented with open circles correspond to the Y XMCD signal and reveal the magnetic behavior of the YFe_2 layers.

from +1 to -1 T, the Dy and Y signals evolve in opposite ways (i.e., the Dy signal increases) whereas the Y one decreases to reach $-Y_{\text{max}}$; (iii) finally, the Dy signal decreases again, whereas the Y signal remains almost constant at $-Y_{\text{max}}$. Moreover, minor loops performed at the Dy edge have shown that the behavior is reversible between +7 and +1 T, but no longer once the DyFe_2 magnetization has switched back along the field direction to follow the YFe_2 magnetization reversal.

From the above observations, the magnetic behavior of the whole superlattice can be described as follows.

(i) The magnetization of YFe_2 is kept stuck along the field direction (referred to as $+z$), while the DyFe_2 magnetization progressively leaves this direction in order to satisfy the antiferromagnetic interface exchange coupling. At 250 K, the situation is such that, close to +1 T, the magnetizations of the layers are in opposite directions. Such a ferrimagnetic configuration minimizes the exchange energy, with a cost in Zeeman energy due to the DyFe_2 magnetization that is opposite to the field direction.

(ii) When the YFe_2 magnetization switches from the $+z$ towards the $-z$ direction, the interface exchange coupling leads to the simultaneous rotation of the DyFe_2 magnetization and thus it comes back to the $+z$ direction. The ferrimagnetic configuration between DyFe_2 and YFe_2 magnetiza-

tion is maintained. At 250 K, the switching of the YFe_2 magnetization starts for negative fields and can thus be attributed to the contribution of the Zeeman energy. However, at 200 K, the YFe_2 reversal starts for positive fields, probably to favor an exchange interaction between iron moments at the interfaces. At this temperature, it is likely more difficult for the DyFe_2 magnetization to turn opposite to the field because both the anisotropy and Zeeman energies are higher.

(iii) For large negative fields, the magnetization in both compounds tends to align along $-z$. As for decreasing positive fields, the YFe_2 magnetization is close to the field direction, whereas the DyFe_2 magnetization is shifted in order to satisfy the exchange interaction. It comes closer and closer to the field direction when the magnitude of the field increases.

Therefore, in contrast to sample I, the DyFe_2 layers behave in this case as softer layers: despite the strong crystal field anisotropy in this compound, the lower Zeeman energy allows the magnetization to shift from the field direction, to satisfy interface exchange interaction. Although other authors¹⁵ have already mentioned the possibility for the magnetic walls to penetrate into the hard material, the results reported in this paper provide direct evidence for such a phenomenon. Moreover, they demonstrate that at 250 K the walls not only penetrate into the hard layers, but are almost completely located in the hard layers, since the YFe_2 magnetization is constant for positive fields.

Figure 4 gathers the magnetization measurements performed at 200 and 250 K with a SQUID magnetometer (solid curves) for the same superlattice, together with the magnetic behavior of the whole superlattices that was deduced from the Y and Dy dichroic signals (open squares) from Fig. 3. The loops with open squares are simply obtained in summing hysteresis loops measured by XMCD at the Dy and Y edges, with a factor of 1.8 between the measured curves (Dy loop + 1.8 Y loop). Let us make clear that no obvious physical conclusion could be deduced from this value of 1.8. Indeed, the amplitude of the dichroic signal measured only at a single partner of the spin-orbit split edge is not directly related to the magnetic moments carried by the absorbing atom. The measured signal depends on many various parameters [e.g., relative thicknesses of the layers, the matrix element of the optical transitions involved ($2p_{3/2}-4d$ or $2p_{3/2}-5d$), number of $4d(5d)$ holes, etc.] Thus we used the same empirical factor in order to obtain the best agreement between the macroscopic- and XMCD-deduced magnetization curves at both temperatures. This analysis allowed us to unravel the details of the magnetization reversal, which was not possible to elucidate from the SQUID hysteresis loops.

In summary, x-ray magnetic circular dichroism measurements performed at the Dy and Y L_3 edges in $\text{DyFe}_2/\text{YFe}_2$ superlattices allows us to obtain element specific information on the magnetic behavior in this composite system. In such heterostructures where the interface exchange coupling may lead to complex and unexpected magnetic configurations, this technique is a precious and unique tool to extract a detailed description of the magnetization reversal. For the

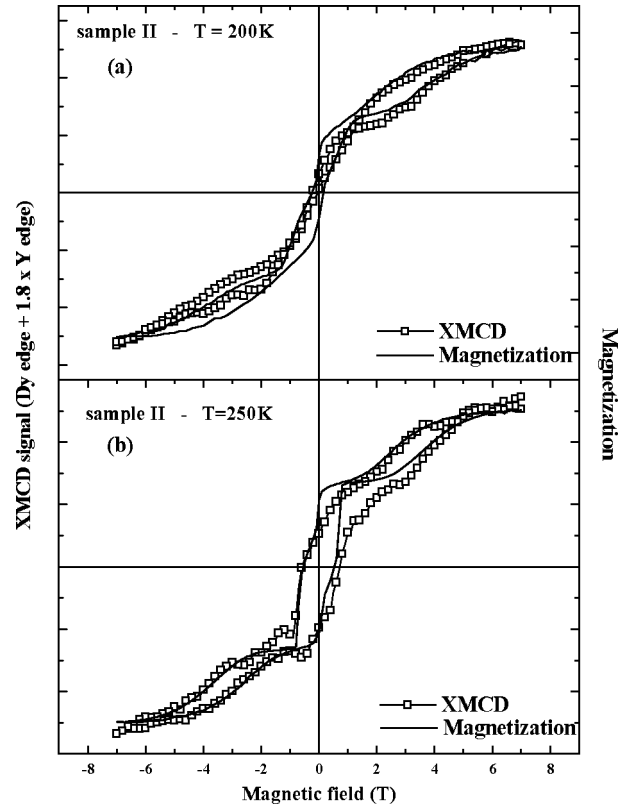


FIG. 4. Hysteresis loops measured at 200 and 250 K for the superlattice $[\text{DyFe}_2(50 \text{ \AA})/\text{YFe}_2(130 \text{ \AA})]_{21}$. The results presented with solid curves correspond to SQUID measurements. The results presented with open squares correspond to a linear combination of the Dy and the Y XMCD signals presented in Fig. 3.

samples investigated in the present study, element-selective hysteresis loops have been measured, which made it possible to investigate the behavior of the magnetic exchange springs. In the superlattice with 50-Å-thick DyFe_2 layers, XMCD measurements reveal that, in contrast to what can be expected from the hard DyFe_2 compound, the exchange coupling leads to the shift of the DyFe_2 magnetization from the field direction, in order to favor the ferrimagnetic configuration between DyFe_2 and YFe_2 layers. The YFe_2 magnetization is essentially aligned with the applied field and governs the DyFe_2 magnetization direction, via interface exchange coupling.

The present study thus demonstrates the necessity to take account of the penetration, or even the location at high temperature, of magnetic springs into the hard layers. Such information is of great interest for a better understanding of exchange coupling related phenomena, such as spring magnet behavior and exchange bias. The further work is in progress to provide a complete description of these systems based on both analytical calculations of the magnetic configurations and detailed studies of the temperature dependence of XMCD signals at both Dy and Y edges for samples with various thicknesses.

- ¹K. Dumesnil, M. Dutheil, C. Dufour, and P. Mangin, *Phys. Rev. B* **62**, 1136 (2000).
- ²S. Wüchner, J. C. Toussaint, and J. Voiron, *Phys. Rev. B* **55**, 11 576 (1997).
- ³S. Mangin, G. Marchal, C. Bellouard, W. Wernsdorfer, and B. Barbara, *Phys. Rev. B* **58**, 2748 (1998).
- ⁴M. Sawicki, G. J. Bowden, P. A. J. De Groot, B. D. Rainford, J. M. L. Beaujour, R. C. C. Ward, and M. R. Wells, *Phys. Rev. B* **62**, 5817 (2000).
- ⁵J. Nogues, D. Lederman, T. J. Moran, and I. K. Schuller, *Phys. Rev. Lett.* **76**, 4624 (1996).
- ⁶E. E. Fullerton, J. S. Jiang, M. Grimsditch, C. H. Sowers, and S. D. Bader, *Phys. Rev. B* **58**, 12 193 (1998).
- ⁷V. Oderno, C. Dufour, K. Dumesnil, Ph. Mangin, and G. Marchal, *J. Cryst. Growth* **165**, 175 (1996).
- ⁸C. T. Wang, B. M. Clemens, and R. L. White, *IEEE Trans. Magn.* **MAG-32**, 4752 (1996).
- ⁹S. Jaren, E. du Tremolet de Lacheisserie, D. Givord, and C. Meyer, *J. Magn. Magn. Mater.* **165**, 172 (1997).
- ¹⁰M. Huth and C. P. Flynn, *Phys. Rev. B* **58**, 11 526 (1998).
- ¹¹A. Mougín, C. Dufour, K. Dumesnil, and Ph. Mangin, *Phys. Rev. B* **62**, 9517 (2000).
- ¹²F. Wilhelm, P. Pouloupoulos, G. Ceballos, H. Wende, K. Baberschke, P. Srivastava, D. Benea, H. Ebert, M. Angelakeris, N. K. Flevaris, D. Niarchos, A. Rogalev, and N. B. Brookes, *Phys. Rev. Lett.* **85**, 413 (2000).
- ¹³J. Goulon, A. Rogalev, C. Gauthier, C. Goulon-Ginet, S. Paste, R. Signorato, C. Neumann, L. Varga, and C. Malgrange, *J. Synchrotron Radiat.* **5**, 232 (1998).
- ¹⁴A. Rogalev, J. Goulon, G. Benayoun, P. Elleaume, J. Chavanne, C. Penel, and P. Van Vaerenbergh, *Proc. SPIE* **3773**, 275 (1999).
- ¹⁵G. J. Bowden, J. M. L. Beaujour, S. Gordeev, P. A. J. de Groot, B. D. Rainford, and M. Sawicki, *J. Phys.: Condens. Matter* **12**, 9335 (2000).